

# Advanced, Independent SRS & SBRT QA Solutions

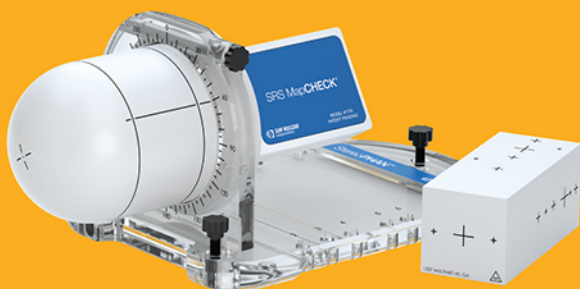
NEW



SunSCAN™ 3D Water Scanning System

Meet the stringent demands of stereotactic treatments, with our suite of SRS/SBRT solutions.

**Learn more:**  
**[sunnuclear.com/srsqa](http://sunnuclear.com/srsqa)**



StereoPHAN™, SRS MapCHECK®, MultiMet-WL Cube



MR Distortion & Image Fusion Head Phantom



STEEV™ Phantom

**[sunnuclear.com](http://sunnuclear.com)**

The SunSCAN 3D system is not available for sale in all markets. CE mark pending.



**SUN NUCLEAR**  
A MIRION MEDICAL COMPANY

# Testing of an enhanced leaf model for improved dose calculation in a commercial treatment planning system

Ann Van Esch<sup>1</sup> | Antti Kulmala<sup>2,3</sup> | Ronan Rochford<sup>4</sup> | Juha Kauppinen<sup>4</sup> | Ari Harju<sup>4</sup>

<sup>1</sup>7Sigma, QA-team in radiotherapy physics, Tildonk, Belgium

<sup>2</sup>Clinical Research Institute HUCH Ltd., Helsinki, Finland

<sup>3</sup>Helsinki University Hospital, Cancer Center, Helsinki, Finland

<sup>4</sup>Varian, a Siemens Healthineers Company, Helsinki, Finland

## Correspondence

Ann Van Esch, 7Sigma, QA-team in radiotherapy physics, Kasteeldreef 2, 3150 Tildonk, Belgium.

Email: [ann.vanesch@7sigma.be](mailto:ann.vanesch@7sigma.be)

## Abstract

**Background:** With the ever-increasing complexity of dynamic radiotherapy treatments, dose calculation algorithms are challenged to accurately calculate the dose resulting from small, on- and off-axis multileaf collimator (MLC) aperture movements. Although the currently available Eclipse (Varian Medical Systems, Palo Alto) dose calculation algorithms still use a simplified, binary MLC model, a more advanced and detailed modeling of the MLC could be beneficial for the dose calculation precision of high-end treatments.

**Purpose:** To improve the modeling of the MLC in the dose calculation algorithms of the Eclipse treatment planning system, an enhanced MLC attenuation model was constructed through ray tracing through the actual leaf designs for the most commonly used Varian MLC types. The enhanced leaf model (ELM) thus includes the rounded leaf tip shape, the drive screw cutout, and the leaf body thickness. The purpose of this work is to test out this new model and explore possible improvements compared to the previous model.

**Methods:** Dose calculations were performed in a research Eclipse environment equipped with the original and enhanced MLC model. Measurements were performed on TrueBeam and on Halcyon dual MLC treatment units. Dedicated static and dynamic MLC test plans were designed to challenge the dose calculation and highlight differences between both models while keeping the experimental setup simple in order to minimize measurement uncertainties. Measurements were performed with single ion chambers, 2D ion chamber arrays and film.

**Results:** The improved MLC model considerably improves the accuracy of the dose calculation for the test fields used in this study. For the TrueBeam MLC, improvements are most prominent for off-axis dose delivery through narrow (static or dynamic) MLC gaps. For 3 mm narrow sweeping gap deliveries at 12 cm off-axis, the advanced model agrees within 2% with the measurement, in contrast to the 12% deviation observed with the original MLC model. For the Halcyon MLC, improvements are especially prominent when the leaves of both MLC stacks are aligned, regardless of their position in the field. Sweeping gap measurements improve from a 7%–10% deviation with the original model to within 2% with the new model.

**Conclusions:** Although test fields designed in this study emphasize the flaws in the original MLC dose calculation model, the enhanced MLC model resolves all of the observed discrepancies, showing excellent on- and off-axis agreements with all of the performed measurements.

## KEYWORDS

dose calculation, dosimetric leaf gap, multileaf collimator

## 1 | INTRODUCTION

When radiotherapy treatments consisted of only conformal static fields, a single transmission parameter was the only parameter used to model the multileaf collimator (MLC) in the Varian (Cadplan/Eclipse) dose calculation algorithms. As intensity-modulated radiotherapy (IMRT) came into use, dose was delivered through dynamic MLC movements, introducing the need to more accurately model the integral dose delivered through sweeping gaps of varying widths. The “dosimetric leaf gap (DLG)” parameter was conceived for this purpose, in theory representing the effective field width of a nominally closed MLC pair with rounded leaf tips.<sup>1</sup> IMRT fields generated by Varian’s leaf motion calculator (LMC) were relatively synchronous left-to-right leaf movements due to the inherent design of the LMC algorithm. The tongue-and-groove effect, typically appearing when neighboring leaf pairs execute highly asynchronous movements, was therefore of limited clinical relevance and ignored in the dose calculation. When the RapidArc (Varian Medical Systems, Palo Alto) optimizer was developed to generate volumetric modulated arc therapy (VMAT) treatments, leaf motions became more chaotic, displaying repetitive back-and-forth trajectories, often of individual leaves. The tongue-and-groove effect present in these delivery patterns could no longer be ignored and was therefore introduced into the dose calculation. Thus, the MLC model evolved into what is currently used by all clinically released photon dose calculation algorithms (up to version v17) in the Eclipse treatment planning. In recent years, stereotactic radiotherapy treatments have been gaining in importance. Although some are treated by conformal arcs, currently, the most common approach within the Varian solution is either through RapidArc or HyperArc VMAT plan optimization. Although single lesions already present a challenge for accurate small field dose calculation, matters are further complicated as single-isocenter multiple-lesion treatments are becoming more and more common practice. Simultaneous treatments of multiple lesions distributed over the whole brain with a single-isocenter treatment plan are no longer exceptional. The leaf movements for these plans consist of mostly closed MLC pairs with the occasional small openings generating the high dose delivery at the location of the lesions. For such high-precision treatments, some centers have reported satisfactory agreement between measured and calculated doses,<sup>2–4</sup> whereas others have found larger differences that were deemed unacceptable.<sup>5–9</sup> The lack of consensus on the precision of the dose calculation suggests that there are multiple possible causes. It is in any case a known fact that small field dose calculations and measurements are both subjected to their own specific challenges. It is beyond the scope of this work to investigate the different possible

culprits. Instead, we aim to focus on the impact of the used MLC model in the dose calculation. More specifically, we aim to evaluate to which extend a more detailed model of the geometric shape of the leaf—describing both the rounded leaf tip design and the leaf thickness profile—can contribute to an improved dose calculation in static as well as dynamic MLC dose delivery.

## 2 | METHODS AND MATERIALS

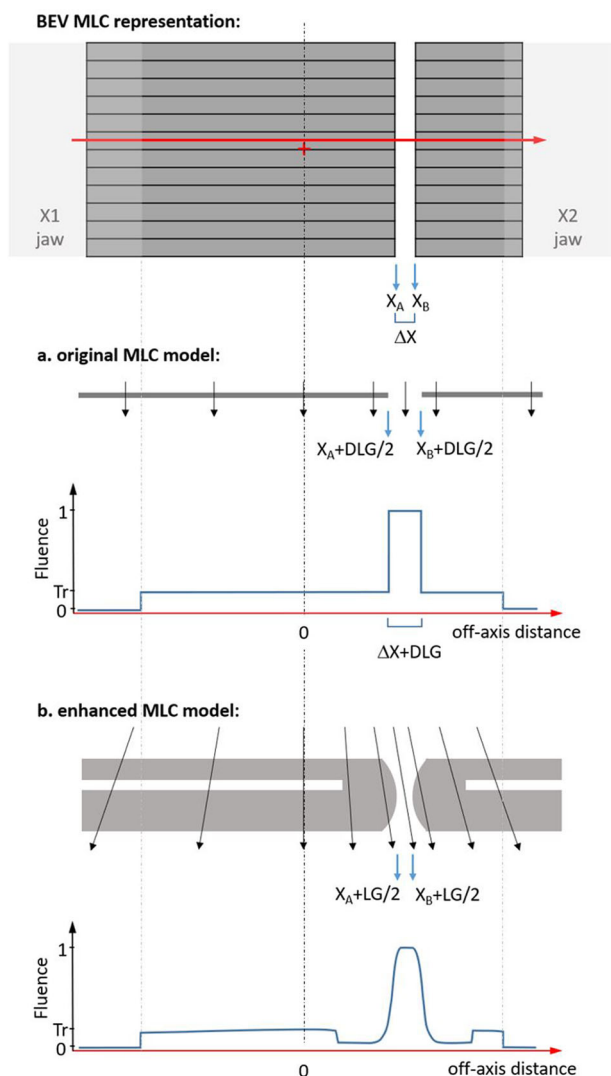
### 2.1 | Theoretical description of the enhanced MLC dose modeling

Figure 1 provides a graphical illustration of both the original MLC model as adopted in the clinically released Eclipse dose calculation algorithms (up to version v17) and of the enhanced leaf model (ELM) presented in this study. For better understanding of both models, dimensions and fluence values are not to scale but are exaggerated for improved visualization.

Dose calculation algorithms in the Eclipse TPS make use of the fluence map that is calculated to represent the intensity of the delivered beam. When the beam is shaped by a (static or dynamic) MLC, the used MLC model directly impacts this fluence calculation.

In the current, simplified MLC model, the MLC is viewed as a thin, homogeneous layer that either attenuates the beam by the set transmission factor or lets the beam pass through unimpeded through its openings. Figure 1a provides a visual illustration of this model for a simple off-axis MLC gap. The two user-definable parameters are the transmission factor ( $T_r$ ) and the DLG. The transmission factor is assumed to be constant over the whole beam. In practice, it is usually measured on the beam axis below the leaf area that has the screw cutout. The dosimetric leaf gap (LG) is used to model the mechanical MLC zero offset as well as the penumbra shift due to the rounded leaf tips: two opposing leaves that have a nominal opening  $\Delta x$  are represented in the fluence calculation as if they have an effective opening  $\Delta x + \text{DLG}$ . Consequently, the fluence representation of a certain MLC gap is the same, regardless of the (off-axis) position of this gap. Below the collimator jaws, the fluence is set to zero.

The ELM no longer represents the MLC as a homogeneous, thin attenuation layer but aims to model its true shape. For the most common MLC types available on Varian treatment units (Millennium 120, HDmlc and the Halcyon dual MLCs), an attenuation model was created based on the leaf design. In the leaf axis direction, the rounded MLC leaf tip shape, the drive screw cutout, and the leaf body thickness are modeled through divergent ray tracing through the leaf. The reference transmission value  $T_r$  is now specifically declared to be the transmission measured on the beam axis below the central



**FIGURE 1** Graphical representation of the fluence calculations with the original (a) and enhanced (b) multileaf collimator (MLC) model for an off-axis MLC gap with nominal opening  $\Delta x$ . (The nominal positions are indicated by  $X_A$  and  $X_B$ .) Dimensions and fluence values are not to scale but exaggerated for improved visualization. DLG, dosimetric leaf gap; LG, mechanical leaf gap among nominally closed leaf tips;  $Tr$ , transmission

leaf area that has the drive screw cutout (as illustrated in Figure 1b) but averaged out over intra- and interleaf transmission. The transmission in all other areas of the MLC is modeled relative to this value. For off-axis positions perpendicular to the leaf direction, the decrease in transmission due to increased path length inside the MLC leaf is now accounted for and different leaf zones (e.g., the 2.5 vs. 5 mm leaves of the HDmlc) are assigned different overall transmission to account for the reduced contribution of interleaf leakage when leaves are wider.  $Tr$  depends on the type of MLC and the energy of the treatment beam. The LG parameter now represents the mechanical calibration and no longer includes the impact of the rounded leaf tip. As mechanical calibra-

tions may still differ among treatment units, this is still a treatment unit-specific parameter. Figure 1b illustrates the enhanced model's impact on the fluence calculation on the narrow off-axis MLC gap in the leaf direction.

## 2.2 | MLC parameter configuration

For the original MLC model in the Eclipse TPS, the most commonly used procedure for deriving the MLC parameters ( $Tr$  and DLG) consists of a transmission measurement in combination with a number of sweeping gap measurements with varying LGs, as originally proposed by LoSasso et al.<sup>1</sup> The TrueBeam's MLC transmission  $Tr$  is obtained through an ion chamber measurement on the beam axis for a  $10 \times 10$  cm<sup>2</sup> collimator field size with the MLC leaf tips fully closed at a 7 cm off-axis position, first to the left (i.e., below X1 [MLC bank A]) and second to the right (i.e., below the X2 jaw [MLC bank B]). The carriage is always forced out of the field by shifting the most caudal leaf pair to the opposite side of the field.  $Tr$  is averaged out over both measurements. By performing the measurement with a large enough ion chamber,  $Tr$  is also averaged out over inter- and intraleaf transmission. The original model's DLG value is obtained through extrapolation to zero dose of the measured dose versus gap size, thus combining the impact of the mechanical LG and the rounded leaf tip shape into one single dosimetric parameter. As an alternative to the extrapolation approach, the DLG value can also be empirically optimized to provide good agreement with the dose calculation for these sweeping gap files. In this study, the latter method was used to obtain the MLC parameters for the original MLC model, but both methods provide comparable DLG values.

To configure the ELM MLC model in the TPS ( $Tr$  and LG), this measurement method can also be used, but the extrapolation approach is no longer suitable as it inherently includes the impact of the leaf tip shape. Rather than going for the empirical, manual optimization, the LG parameter is now iteratively fitted by the beam configuration software to provide optimal agreement between the measured and ELM-calculated dose for a selection of sweeping gap deliveries. Three sweeping gaps are used per MLC type. Sweeping gaps of 4, 6, and 20 mm in a  $10 \times 10$  cm<sup>2</sup> collimated field are used for the HDmlc and Millennium 120. For the Halcyon's stacked MLC, a 5 mm sweeping gap is analyzed per individual MLC and with both MLCs performing the movement simultaneously. Transmission measurements are identical to the ones performed for the original model, but the resulting  $Tr$  value is now declared to be the transmission value below the central part of the leaf that has the screw cutout.

The transmission and sweeping gap measurements were performed at isocenter in a water phantom (Blue Phantom, IBA Dosimetry, Schwarzenbruck, Germany)



at 10 cm depth. A large volume ion chamber (NE2571 Farmer 0.6 cm<sup>3</sup>) was used to assure adequate averaging over inter- and intraleaf transmission.

## 2.3 | Experimental verification of the ELM dose calculation

Although the validation of the ELM model was performed on a variety of treatment units with different MLC types and multiple energies, in this publication, we primarily restrict ourselves to measurements performed in the HUCH Hospital (Comprehensive Cancer Center, Helsinki, Finland) on the 6 MV treatment beam of an HDmhc TrueBeam and on the 6FFF treatment beam of a Halcyon to provide a representative yet comprehensive illustration of the observed changes in dose calculations. The MLC parameters were also determined for the other photon energies on the TrueBeam treatment units to test the consistency of the LG value, regardless of the beam energy. All dose calculations were performed with the Acuros (v17) dose calculation algorithm in an Eclipse test environment equipped with both the original and a developer prototype for the ELM model. Calculation resolution was set to 0.1 cm, unless stated otherwise. All beam data were configured to obtain an absolute dose calibration of 1 cGy/MU with a 10 × 10 cm<sup>2</sup> field at isocenter at source-skin-distance SSD = 95 cm (i.e., at depth = 5 cm). In theory, the spot size parameters (SpotX and SpotY) in the beam configuration model represent the size of the focal spot of the electron beam as it hits the target. In clinical practice, however, on TrueBeam treatment units, these parameters have often been used as empirical tuning factors in the beam configuration environment, either to improve small field CAX dose calculations or to try and match the calculated penumbra shape to measurements, either to the MLC leaf tip penumbra (SpotSizeX) or to the jaw penumbra. In order to purely focus on the impact of the enhanced versus original MLC leaf tip model, this additional tuning should be omitted. The spot sizes of the 6 MV TrueBeam photon beam were thus set to values representing the actual physical dimensions (SpotX = 0.05 cm, SpotY = 0.07 cm).<sup>10</sup> For the Halcyon 6FFF photon beam, no user-specific modification of the clinically released preconfigured datasets is allowed. The original MLC model was therefore evaluated with the spot size dimensions as defined in the original dataset (SpotX = 0.07 cm, SpotY = 0.07 cm). The ELM model was evaluated with dimensions that better approximate the Halcyon's physical spot size (SpotX = 0.12 cm, SpotY = 0.18 cm).

Static fields were used to assess the ability of the ELM model to better represent the overall MLC transmission and the shape of the rounded leaf tip in the dose calculation. Dynamic fields were used to assess the impact on the integral dose. To minimize random

impact of possible MLC movement backlash, for all of the below measurements, the MLC was positioned at a starting position to the far left before moving to its treatment position. The field size in the Y-direction was set to 20 cm to include a large number of leaves (Y = 20 cm) and thus involve more leaves than merely the ones used for parameter optimization. All validation measurements were performed in solid water (PTW, Freiburg) at 10 cm depth at SSD = 90 cm. For every measurement setup, at least two measurement methods were used as a double-check or to provide complimentary information. Ion chamber array measurements (Octavius 1500 or stereotactic 1600SRS array, PTW, Freiburg) and single ion chamber measurements were always cross-calibrated to the expected dose for a 10 × 10 cm<sup>2</sup> field (100 MU) at isocenter to eliminate all possible imprecisions due to treatment unit's daily output, imperfect water equivalence of the solid water, and slight imprecisions in the measurement setup. When high-resolution or accurate absolute dose levels for small beam aperture were needed, radiochromic film measurements were included (GafChromic EBT3, Ashland Inc., Covington, KY). Film measurements were repeated three times to average out random measurement uncertainty. On the fourth day after irradiation films were digitized using a Vidar dosimetry pro advantage (Vidar Systems Corporation, Herdon, VA) densitometer and nonlinearity of the densitometer's lateral response was corrected. Conversion from optical density to dose was made using a calibration curve defined for the film lot on the measurement session. Film measurement results have nominal resolution 0.1 mm.

To ensure measured data are averaged out over inter- and intraleaf transmission, profiles extracted from array measurements were always averaged out over a number of detector rows. For the 1500 Octavius array, averaging out over three rows (or columns) corresponds to a 1.5 cm wide area. Averaging out over five rows covered a 1.25 cm wide data selection for the 1600SRS stereotactic array. Film measurements were averaged out over a width of 1 cm.

### 2.3.1 | 2D MLC transmission

Although the transmission measurement for the model configuration was performed with a single ion chamber on the beam axis, the off-axis modeling of the MLC transmission of the HDmhc was assessed through measurement with a 2D array (Octavius 1500, PTW, Freiburg). The phantom and array were shifted 10 cm laterally to allow the array's surface (27 × 27 cm<sup>2</sup>) to cover an asymmetric field (X1 = -2 cm, X2 = 16 cm, Y = 20 cm, 500 MU) with the MLC fully closed as depicted in the insets of Figure 2. The leaf tips are closed below the X1 jaw, at a 1 cm distance from the jaw's edge, except for the most caudal leaf pair that is

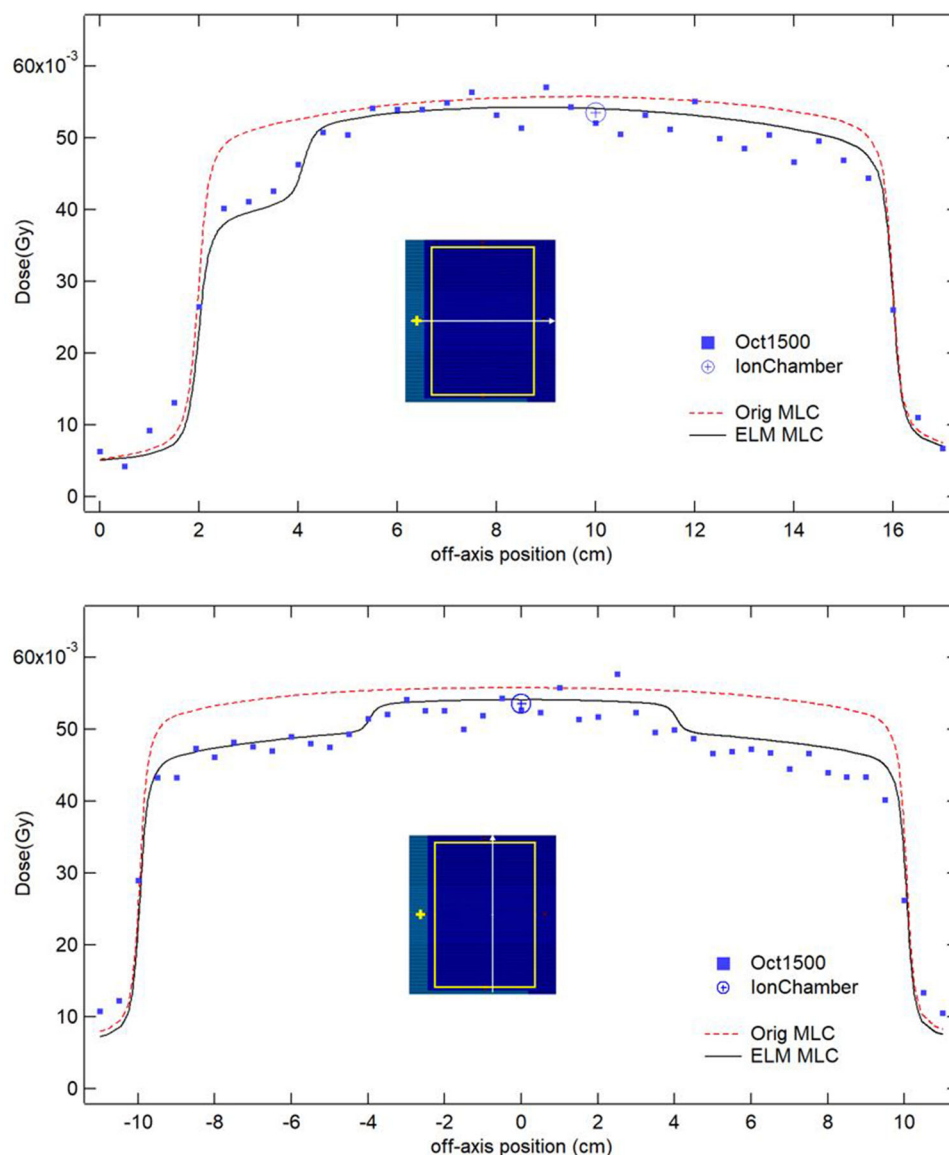


**FIGURE 2** Measured and calculated orthogonal dose profiles for a fully closed, asymmetrical HDmlc field ( $X1 = -2$  cm,  $X2 = 16$  cm,  $Y = 20$  cm, 500 MU) as depicted in the insets. The measured profiles (blue squares) were extracted from two merged planar measurements with the Octavius 1500 ion chamber array and averaged out over a width of 1.5 cm (three detector rows/columns). Dose calculations were performed with the original and enhanced leaf model (ELM) multileaf collimator (MLC) model. The single ion chamber (crossed blue circle) was made with a SemiFlex 0.125 cm<sup>3</sup> ion chamber, positioned at 10 cm off-axis (lateral). Dose calculation results for the original (dashed redline) and the enhanced leaf model (solid black line) are shown.

shifted to the other side of the field to force the MLC carriage out of the beam aperture. A second measurement was performed with the array shifted by 0.5 cm in the longitudinal direction. As each measurement set provides a checkerboard pattern of datapoints (with a 1 cm center-to-center distance), the merging of both measurements results in near-full coverage of the measured surface, with a spatial resolution of  $0.44 \times 0.44$  cm<sup>2</sup> per measurement point. An additional single ion chamber measurement with a 0.125 cm<sup>3</sup> SemiFlex (31010) (PTW, Freiburg) was performed in the 10 cm off-axis position to double-check the correct absolute level of the array

measurement. Dose calculations (resolution = 2.5 mm) were performed with both MLC models.

### 2.3.2 | Static wallpaper

In large-field static deliveries, the exact shape and position of the leaf tip penumbra is of significance in areas where subsequent MLC segments form junctions. To study the dosimetric impact at the location of the junction itself, plans were made consisting of adjoining static rectangular MLC deliveries that together cover a

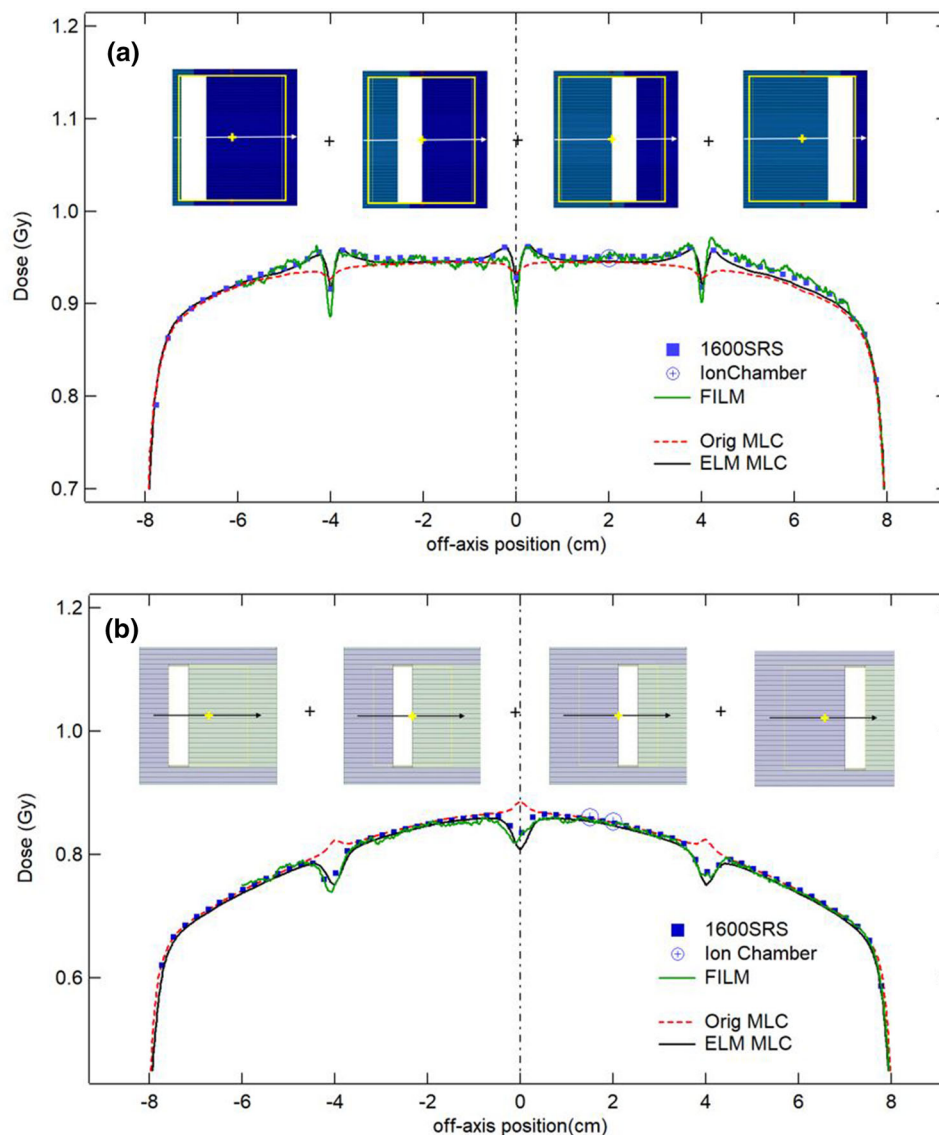


**FIGURE 3** Measured and calculated dose profiles along the leaf direction for the static wallpaper delivery for an HDmlc (a) and Halcyon dual multileaf collimator (MLC) (b). Calculations were performed with the original (red dashed red line) and enhanced leaf model (ELM) (solid black line) MLC model. The 1600SRS data (blue squares) are merged from multiple laterally shifted acquisitions. Film data (solid green line) were averaged over three repeated measurements films. The single ion chamber (crossed blue circle) confirms the correct absolute dose level.

larger surface, much like wallpaper covers a wall. For the TrueBeam, the nominal MLC apertures were programmed to show some slight overlap in order to avoid pronounced dose peaks at the junction. For the MLC used in this work, an overlap of 0.3 mm provided a delivery that comes close to a perfect junction according to the original MLC model. For the Halcyon MLC, both MLCs were programmed identically, and no overlap between subsequent segments was foreseen. Again, a BEV representation of the delivery is given in the insets of Figure 3 for the TrueBeam (a) as well as for the Halcyon (b). Dose calculations were performed with 100 MU/segment. Measurements were performed both with the stereotactic 1600SRS ion chamber matrix

(PTW, Freiburg) ( $0.25 \times 0.25 \times 0.05 \text{ cm}^3$ ) and with film to obtain high spatial resolution at the level of the junctions. Subsequent deliveries whereby the matrix was shifted laterally allow us to reconstruct the entire irradiated area at full detector surface coverage. Films strips were cut to size to include all junctions into the measurement area. Film measurements were performed with higher MUs to obtain optimal film density and rescaled to the calculated MUs afterward. An additional single ion chamber (SemiFlex3D (31021), PTW, Freiburg) measurement was performed at a 2 cm lateral off-axis position (i.e., in the center of one of the strips) to provide an absolute dose reference level.

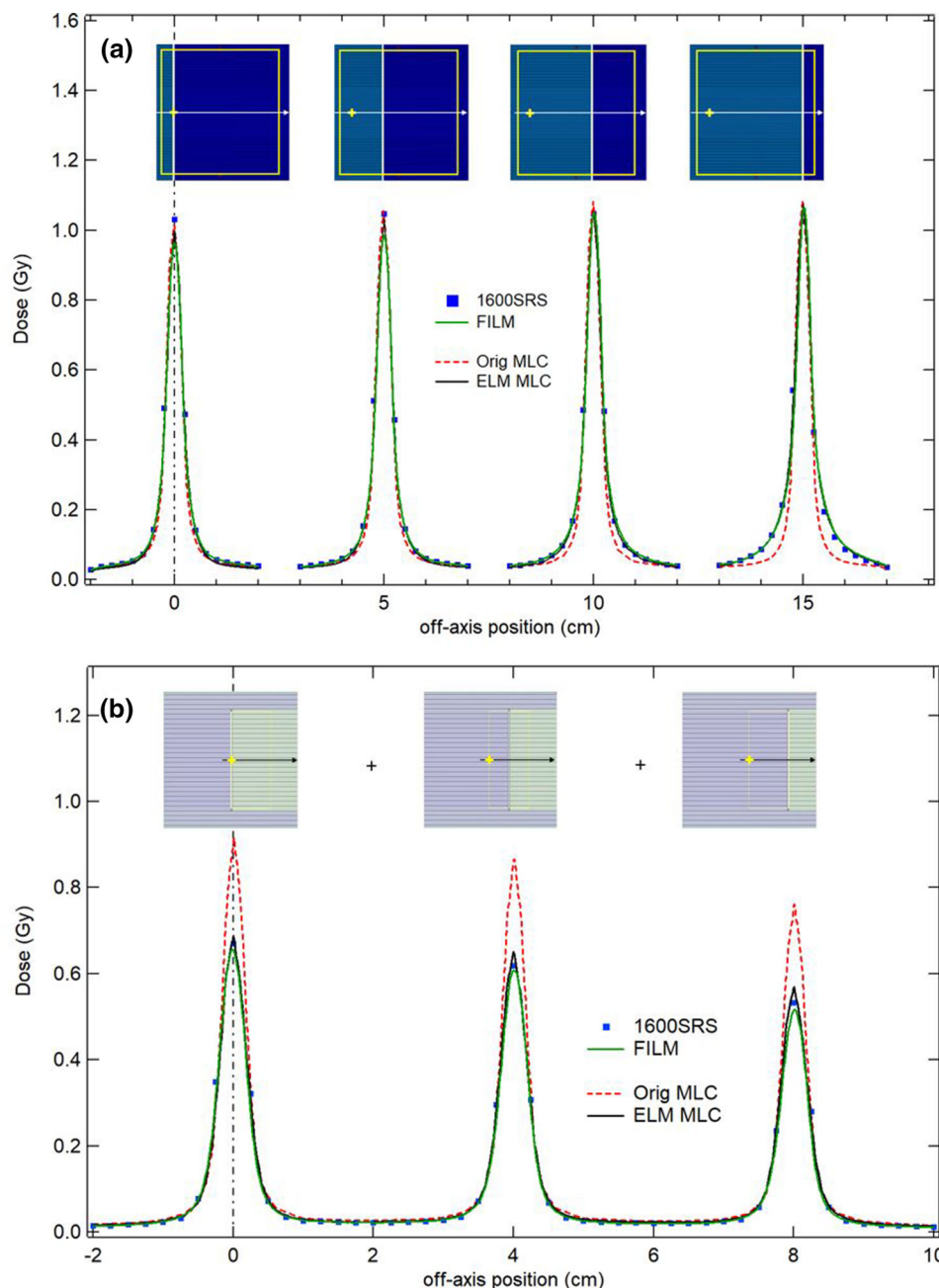


**FIGURE 4** Measured (film: solid green line and 1600SRS: blue squares) and calculated (original: dashed redline and enhanced leaf model [ELM]: solid black line) dose profiles for static narrow multileaf collimator (MLC) strips (nominal gaps of 3 mm wide, on- and off-axis, 200 MU/strip). On the TrueBeam (a), each strip is calculated and measured individually. On the Halcyon (b), the strips are merged into a single step-and-shoot delivery.

### 2.3.3 | Static narrow MLC strips

A second assessment of the impact of the detailed modeling of the leaf tip shape on the precision of the dose calculation was performed by means of narrow static MLC strips, both on- and off-axis. On the TrueBeam, 3 mm wide slits were located on the beam axis and at 5, 10, and 15 cm off-axis, respectively, as shown in the inset of Figure 4a. On the Halcyon, 3 mm slits (shaped by both

MLCs simultaneously) were placed 0, 4, and 8 cm off-axis (inset of Figure 4b). All calculations were performed with 200 MU/strip. On the TrueBeam, each strip was calculated and measured separately. On the Halcyon, the three strips were merged into a single step-and-shoot delivery. Measurements were performed with the stereotactic 1600SRS 2D-array and with film. For each strip measurement on the TrueBeam, the 1600SRS array was shifted laterally in order to ensure that the central



part of detector (where detector density is such that it provides full surface coverage) was positioned below the strip. For the Halcyon, multiple shifted acquisitions were again merged. Again, film measurements were performed with higher MUs to obtain optimal film density and rescaled accordingly for comparison with the array measurements and calculations.

### 2.3.4 | Dynamic zebra crosswalk

Given the prominent role of IMRT and VMAT treatments in current day radiotherapy, test plans were also designed to study the impact of the ELM model on the integral dose during dynamic delivery. As changes are especially expected to occur off-axis and/or for narrow MLC aperture delivery, a fluence pattern was created in the shape of a zebra crosswalk, delivering dose at different off-axis areas through narrow sweeping gap openings. Stripes were centered around the beam axis and at 4, 8, and 12 cm off-axis. For the TrueBeam HDmlc, all stripes were designed to have a final width of 2 cm, and each was delivered as an individual field with a sweeping gap width of 3 mm. On the Halcyon, the entire crosswalk pattern was created as a single field, consisting of 1.5 cm wide integral dose deliveries delivered through 5 mm sweeping gaps. In between these stripes, the dose rate was dropped to minimize dose. A BEV representation is given for both MLCs in Figure 5.

Measurements were performed with the 1600SRS array, again shifted, and merged for maximal detector surface coverage. An additional independent ion chamber measurement (SemiFlex3D) was performed at the center of each stripe to double-check the absolute dose level. Based on the manufacturer's listed small field correction factors<sup>11</sup> (updated to include the TRS 483 code of practice), no additional small field correction factors were applied.

## 3 | RESULTS

### 3.1 | MLC parameter configuration

Single ion chamber transmission and sweeping gap measurements resulted in the MLC parameters are listed in Table 1. For the HDmlc 6 MV beam, a measured transmission value of 0.012 was used for both models, the DLG was optimized to 0.054 cm and the LG to −0.038 cm. The LG values obtained for the other energy beams on the same treatment unit ranged between −0.037 and −0.047 cm, all agreeing within 0.01 cm with the 6 MV value. The Halcyon transmission and DLG values remained those from the preconfigured, clinically released v17 beam dataset ( $Tr = 0.0047$ ,  $DLG = 0.01$  cm). The Halcyon's LG value was iterated to −0.065 cm.

**TABLE 1** Multileaf collimator (MLC) parameters derived from single ion chamber transmission and sweeping gap measurements in a water phantom

	Tr	DLG (cm)	LG (cm)
HDmlc (6 MV)	0.012	0.054	−0.038
HDmlc (6FFF)	0.010	0.047	−0.047
HDmlc (10 MV)	0.013	0.066	−0.037
HDmlc (10FFF)	0.012	0.063	−0.043
Halcyon (6FFF)	0.0047	0.01	−0.065

Abbreviations: DLG, dosimetric leaf gap; LG, leaf gap; Tr, transmission.

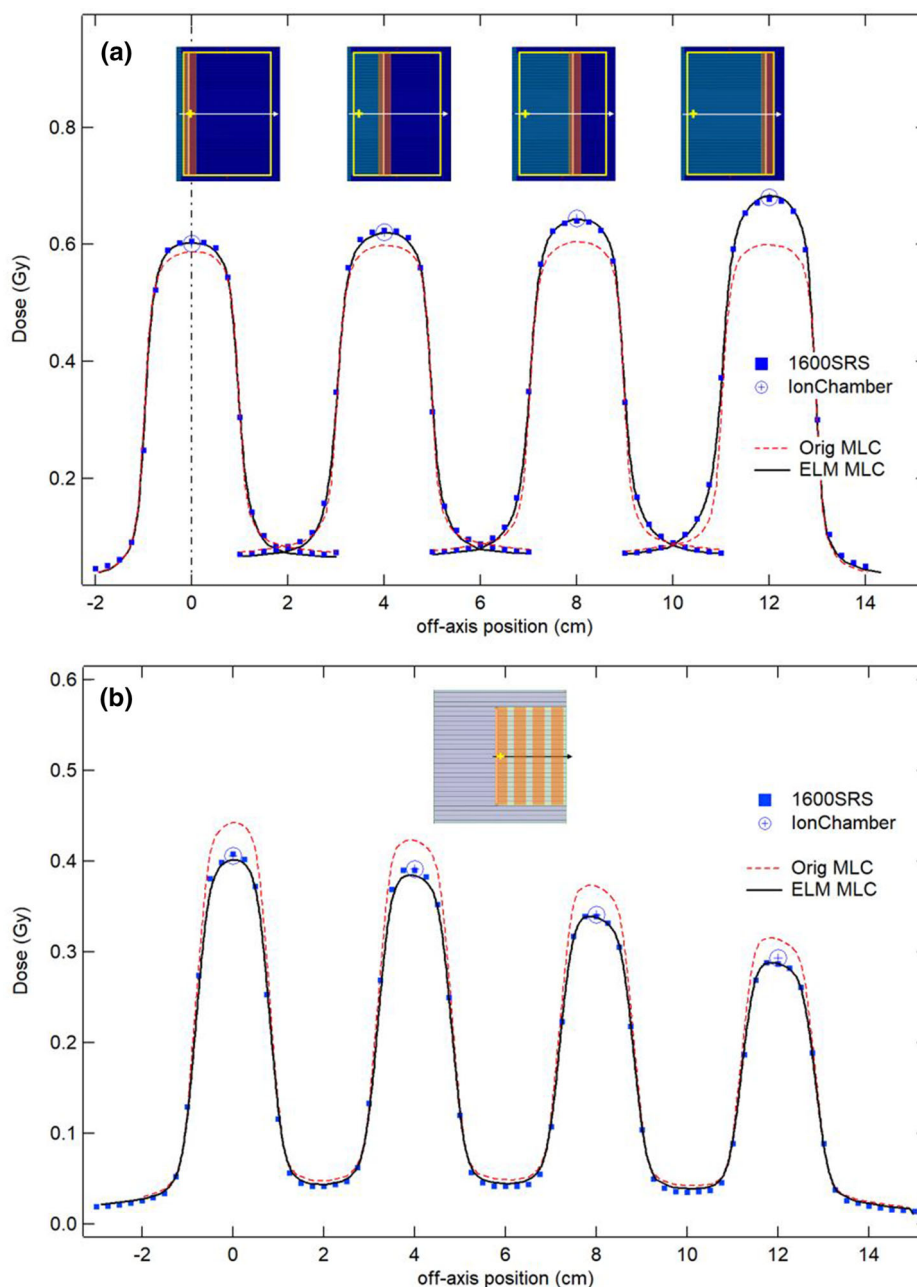
### 3.2 | 2D MLC transmission

Figure 2 compares the measured and calculated dose for the off-axis, closed HDmlc setup through line profiles extracted from the merged 2D measurements. In the transversal profile, the clear difference that can be seen in the measurement between the solid leaf end and the screw drive cavity is well represented in the ELM dose calculation. As the off-axis distance increases, the ELM model also shows the gradual decrease in transmitted dose as the path length through the leaves increases. Both these effects are absent in the original calculation that models the dose as a homogeneous field with the absolute level simply defined by the transmission measured on the beam axis. In the longitudinal direction, the ELM calculation displays the lower overall dose in the MLC area covered by the larger leaves, whereas the original model ignores the difference between both zones.

### 3.3 | Static wallpaper

The impact of the exact leaf tip shape on junctions is visible from the results shown in Figure 3. Although the original MLC model predicts near-invisible junctions among the adjoining segments of the HDmlc, measurements show that in reality the smoothest possible junctions still display slight dose bumps around a central dip. This distinct shape is also discernible in the ELM dose calculation. For the Halcyon MLC, the discrete dose peaks calculated by the original MLC model at the level of the junctions are not confirmed by the measurements. On the contrary, the junctions display an unmistakable dip in the dose level that is again well represented by the ELM dose calculation. The accumulated effect of the overlapping penumbras in the wallpaper pattern is visible for all junctions, whether on- or off-axis.

The independent single ion chamber measurement confirms the correct absolute dose level of both the film and the 1600SRS measurement. At the level of the junctions, the high-resolution film shows more pronounced peaks and dips than the array measurements,



**FIGURE 5** Measured (1600SRS: blue squares and ion chamber: blue circles) and calculated (original: dashed redline and enhanced leaf model [ELM]: solid black line) transversal profiles of the dynamic zebra crosswalk delivery. On the TrueBeam, each stripe was calculated, delivered, and measured individually. On the Halcyon, all stripes were calculated, delivered, and measured as a single dynamic field. Multiple, shifted 1600SRS measurements (blue squares) were acquired on both treatment units and merged where necessary. Single ion chamber measurements were performed with a Semiflex 3D (31021) (crossed blue circles).

but both agree well with the ELM dose calculations (0.1 cm calculation resolution).

### 3.4 | Static narrow MLC strips

For the static, narrow MLC strips, the film data are considered to be the reference measurements, especially regarding the absolute level of the dose peaks. Although

some caution regarding the absolute precision of narrow peaks is advisory when solely relying on a 1600SRS array, for our case, 2D array and film measurements are in very good agreement. For the HDmlc (Figure 4a), the height of the strips is correctly (within 3%) calculated by both models. The effect of the improved MLC model is mostly seen in the penumbra and low-dose areas just outside the strips. The original model agrees well with the measurements for the central strip, but deviations in

the lower part of the peaks increase in magnitude as the strip moves further off-axis. The ELM model calculates the narrow dose strips equally well for on- and off-axis positions, as can be seen for the 10 and 15 cm off-axis positions in particular.

On the Halcyon treatment unit, film and array measurements are again in good agreement. But the impact of the ELM model on the Halcyon dose calculation (Figure 4b) is distinctly different from the one on the HDmlc: in the low dose areas, no noticeable deviations are observed between the measurements and either of the dose calculation models. However, the use of the ELM model exhibits a drastic change in the height of the dose peaks, which now coincide within 4% with the measurement, compared to the more than 30% deviation observed for the original MLC model.

### 3.5 | Dynamic zebra crosswalk

Single ion chamber and 1600SRS measurement data are in good agreement (within 1% on the HDmlc and within 2% on the Halcyon). For the dynamically delivered zebra crosswalk pattern with the HDmlc, comparison between measurements and dose calculations with the original MLC model show increasing deviations with increasing off-axis distance. Although the 3% difference for the on-axis stripe can still be considered acceptable, off-axis stripes reveal 4%, 6%, and 12% absolute dose differences for the 4, 8, and 12 cm off-axis stripes, respectively (Figure 5a). The ELM dose calculation model reduces these deviations to within 1% for all stripes. The improved ELM dose calculation in the penumbra is less prominent than in the static test fields of Figure 4a but can be observed even so, for example, on the left side of the 12 cm off-axis peak. The right side of this stripe does not show any change among the different dose calculation models as it is shaped by the X2 jaw instead of the MLC.

Synchronized movement of the dual layer MLC of the Halcyon treatment unit leads to a systematic overestimation of the integral dose within the zebra crosswalk stripes when using the original MLC model. Local dose deviations of 7%–10% are observed. The ray-tracing dual MLC model reduces these deviations to below 2%, regardless of the off-axis position of the stripe.

## 4 | DISCUSSION

The official procedure for obtaining the MLC parameters in the clinically released Eclipse dose calculation algorithms is based on the sweeping gap extrapolation as originally proposed by LoSasso<sup>1</sup> for the implementation of IMRT treatments. Since then, treatments have evolved to VMAT delivery, characterized by more unsyn-

chronized MLC movements, and stereotactic delivery, characterized by very narrow MLC openings. In addition, single-isocenter multiple metastasis VMAT treatments combine challenges of both VMAT and stereotactic treatments: relatively chaotic MLC movements with small, off-axis MLC openings. As dose calculation, treatment delivery, and treatment QA are being pushed to their limits, discrepancies between measured and calculated doses have been reported. A number of publications advocate the empirical tuning of MLC parameters according to the used treatment technique in order to optimize agreement between measured and calculated patient QA<sup>5-9,12</sup>. Some create a separate beam dataset with MLC parameters tuned to be used only for stereotactic deliveries. Some tune their overall MLC parameters for VMAT delivery to simply obtain better agreement with their specific patient QA system of choice. Still, most centers stick to the official procedure for MLC parameter determination based on the sweeping gap CAX measurements as the fiddling with the MLC parameters is a very empirical approach that does not address the question whether or not the MLC model is the true cause of the observed deviation. Although the original MLC model in the dose calculation may be part of the reason behind unsatisfactory QA results, numerous other possible culprits must not be ignored (measurement detector system uncertainty such as field size, dose rate, and directional dependence), inadequate algorithm configuration, imprecise measurement setup, mechanical and/or dosimetric treatment delivery imprecisions (jaw calibration, isocentric imprecision, beam centering, MLC lag, and so on), and so on.

The test fields in this study were deliberately designed to isolate the impact of the MLC model in the dose calculation algorithm from the other possible causes. Measurement uncertainties were reduced to a minimum by restricting ourselves to simple, orthogonal, large jaw field setups for which well-established measurement methods could be used. All measurements were performed with the ion chamber array that was deemed most suitable, but every one of those measurements was independently validated/supplemented with at least one additional measurement. Although the 1600SRS provides an easy, reliable, and reproducible high-resolution, high detector density measurement, its liquid-filled detectors have a  $0.25 \times 0.25$  cm<sup>2</sup> surface area and a slight field size dependence.<sup>3,13</sup> By choosing a  $10 \times 10$  cm<sup>2</sup> field size for the cross-calibration procedure, we aimed to adequately eliminate the impact of the field size dependence for most of the artificial field geometries used in this study. The independent ion chamber point dose verifications confirmed this supposition. To address the effect of the 0.25 cm detector size, film measurements were added as the golden standard when high-resolution or small aperture absolute dose data were needed.

Although the mechanical LG for the ELM model could in theory be obtained through a physical measurement with a feeler gauge, this measurement is tedious to perform, subject to interpretation, and does not provide the desired precision. The sweeping gaps on the other hand have proven to be robust and easy to perform measurements that are highly sensitive to the mechanical MLC calibration. It is therefore only logical to yet again rely on these for LG parameter optimization. The automated ELM MLC parameter configuration based on the selected point measurements provided transmission and LG values that were in agreement with what was obtained through manual parameter optimization. Although DLG values have always been positive values, the LG parameter can be—and often is—slightly negative. This is inherent to the automated procedure used for the MLC calibration. The leaves of opposing leaf banks are driven forward until a collision is detected. The system only recognizes a collision when the leaf position read out no longer changes, despite increased tension in the leaf drivetrain system. This means that when the leaves are said to collide, they are actually already a small amount beyond collision, hence the negative sign of the automatically set LG. Feeler gauge measurements confirm this: between the leaf tips of an MLC with a negative LG, no feeler gauge can be inserted until the opening exceeds the absolute value of the negative LG parameter. The LG values obtained for different energies on the same treatment unit were all within 0.01 cm of the value obtained for the 6 MV beam, strengthening the hypothesis that the LG value is a mechanical parameter describing the offset of the MLC and should therefore be independent of the beam modality.

From the obtained results with the automatically configured ELM MLC parameters, it can be irrevocably concluded that the enhanced model results in dose calculations that are superior to the ones obtained with the original model as presented in Figure 1. For the (static and dynamic) cases that highlight the inadequacies of the original model, excellent agreement is obtained between measured and ELM calculated dose distributions. The overall effect of the ray-tracing model compared to the simple, homogeneous MLC model is noticeably different between the TrueBeam's single and the Halcyon's dual MLC system.

As the transmission is a non-negligible component of the delivered dose through the TrueBeam's MLC, the improvements in the dose calculation come from both the improved 2D transmission lookup table and the rounded leaf tip ray tracing. The static, closed MLC field illustrates exclusively the first. The wallpaper junctions and narrow strips are a manifestation of the second. The considerable improvement in the dynamic zebra crosswalk pattern dose calculation is a combination of both. Both improvements primarily impact the off-axis dose calculation for very narrow MLC beam aperture delivery. Close to the beam axis, differences between

the original MLC model and the ELM model are minimal. It thus follows that tweaking the MLC parameters to obtain better off-axis agreement for the original model inevitably deteriorates the results in the central part of the beam and vice versa. The exact impact of the MLC model improvements on clinical plans is difficult to predict as it depends on the exact leaf motions. Even so, we can state that, for the exact same delivery, dose calculations with the ELM model will either be similar to or higher than the dose calculations with the original MLC model, depending on the relative contributions from on- and off-axis, narrow MLC gap deliveries.

The transmission contribution to the total dose on the Halcyon dual MLC system is much smaller than that of an MLC on a TrueBeam (or Clinac). Improvements in the 2D MLC transmission therefore hardly impact the overall dose calculation for the Halcyon MLC. The most prominent improvement comes from the ray tracing through the double leaf tips. For the original, thin layer MLC model, it makes no difference whether a LG is shaped only by the upper, only by the lower or by both MLCs simultaneously: the fluence peak representing the LG opening (Figure 1a) will be of identical width and height in all three cases. When ray tracing through the actual leaf tips, however, this is no longer the case. When stacked leaf tips are aligned, the combined focalization of both MLCs results in a different penumbra and a reduction of the total photon flux passing through a narrow MLC opening. This was also recently studied and reported by Azorin et al.<sup>14</sup> The impact of this is visible in all test plans, from the improved modeling of the junction in the wallpaper composite delivery to the reduction in the dose peak of the narrow static slits, to the very significant and unmistakable drop in the integral dose of the sweeping gap zebra crosswalk pattern. Although not elaborated on in this manuscript for the sake of simplicity, the impact of the change in spot size between both dose calculation algorithms was also investigated. Increasing the SpotX parameter from 0.07 to 0.12 cm had no noticeable impact on the wallpaper or zebra crosswalk dose calculations, but, for good measure, it needs to be stated that for the narrow strips, the reduction in the height of the calculated dose peaks is not solely the result of the ELM model but can partly be attributed to the use of a larger spot size (SpotX). Although the ELM model significantly improves the dose calculation for these test cases, it is difficult to predict the impact for clinical plans. In clinical plans, the stacked MLCs are less likely to move in perfect alignment as asynchronous movement of the MLC leaves allows for enhanced geometric resolution in the optimization process. If synchronous movement is to occur, it is most likely to happen in IMRT sweeping gap deliveries when leaf movement is more synchronous by nature. Using the ELM dose calculation model instead of the original MLC model will ensure an improved dose calculation.



## 5 | CONCLUSION

An enhanced MLC model based on the actual leaf design was developed for the most common MLC types available on Varian treatment units (Millennium 120, HDmlc and the Halcyon MLCs). Dedicated test plans designed to highlight the flaws in the original MLC model show excellent agreement between measurements and dose calculations with the new ELM model, indicating that treatment-type specific MLC parameter optimization should no longer be necessary nor advisable. For the TrueBeam MLCs, improvements mostly concern off-axis delivery with small MLC openings (static or dynamic). For the Halcyon dual MLC, the enhanced model drastically improves dose calculations when the MLC leaf tips of both MLCs are (statically or dynamically) aligned.

## ACKNOWLEDGMENTS

The authors would like to thank PTW (Freiburg, Germany) for the fruitful collaboration and for providing dosimetric equipment. 7Sigma and HUCH both have a research collaboration with Varian Medical Systems.

## CONFLICT OF INTEREST

The authors have no relevant conflicts of interest to disclose.

## FUNDING INFORMATION

None.

## REFERENCES

- LoSasso T, Chui C, Ling C. Physical and dosimetric aspects of a multileaf collimation system used in the dynamic mode for implementing intensity modulated radiotherapy. *Med Phys*. 1998;25(10):1919-1927. <https://doi.org/10.1118/1.598381>
- Fogliata A, Nicolini G, Clivio A, Vanetti E, Cozzi L. Accuracy of Acuros XB and AAA dose calculation for small fields with reference to RapidArc® stereotactic treatments. *Med Phys*. 2011;38(11):6228-6237. <https://doi.org/10.1118/1.3654739>
- Van Esch A, Sergent F, Basta K et al. Implementing stereotactic RapidArc treatments into clinical routine: from algorithm configuration to treatment validation. *Med Phys Int J*. 2017;5(1):95-116. <https://doi.org/10.1016/j.ejmp.2017.10.109>
- Fogliata A, Lobefalo F, Reggiori G et al. Evaluation of the dose calculation accuracy for small fields defined by jaw or MLC for AAA and Acuros XB algorithms. *Med Phys*. 2016;43(10):5685. <https://doi.org/10.1118/1.4963219>

- Kielar K, Mok E, Hsu A, Wang L, Luxton G. Verification of dosimetric accuracy on the TrueBeam STx: rounded leaf effect of the high definition MLC. *Med Phys*. 2012;39:6360-6371. <https://doi.org/10.1118/1.4752444>
- Szpala S, Cao F, Kohil K. On using the dosimetric leaf gap to model the rounded leaf ends in VMAT/RapidArc plans. *J Appl Clin Med Phys*. 2013;15:67-84. <https://doi.org/10.1120/jacmp.v15i2.4484>
- Middlebrook ND, Sutherland B, Kairn T. Optimization of the dosimetric leaf gap for use in planning VMAT treatments of spine SABR cases. *J Appl Clin Med Phys* 2017;18(4):133-139. <https://doi.org/10.1002/acm2.12106>
- Jinkoo K, James H, Ting HA, Shidong L, Zhigang X, Samuel R. Relationship between dosimetric leaf gap and dose calculation errors for high-definition multi-leaf collimators in radiotherapy. *Phys Imaging Radiat Oncol*. 2018;5:31-36. <https://doi.org/10.1016/j.phro.2018.01.003>
- Vieilleveigne L, Khamphan C, Saez J, Hernandez V. On the need for tuning the dosimetric leaf gap for stereotactic treatment plans in the Eclipse treatment planning system. *J Appl Clin Med Phys*. 2019;20(7):68-77. <https://doi.org/10.1002/acm2.12656>
- Sawkey D, Constantin M, Mansfield S, et al. Measurements of electron spots on TrueBeam. *Med Phys*. 2013;40(6):332. <https://doi.org/10.1118/1.4814982>
- PTW code of practice for small field dosimetry. p 33. Accessed February 14, 2022; <https://www.ptwdosimetry.com/en/support/downloads/?type=3451&downloadfile=1836&cHash=f4027478a0444987243a730991d2ed1c>
- Miyasaka R, Cho S, Hiraoka T et al. Investigation of Halcyon multi-leaf collimator model in Eclipse treatment planning system: a focus on the VMAT dose calculation with the Acuros XB algorithm. *J Appl Clin Med Phys*. 2022;23(3):13519-13529. <https://doi.org/10.1002/acm2.13519>
- Prabakar S, Mc Callum CD, Hounsell R, McGarry CK. Characterisation of a two-dimensional liquid-filled ion chamber detector array using flattened and unflattened beams for small fields, small MUs and high dose-rates. *Biomed Phys Eng*. 2016;2(2):025007. <https://doi.org/10.1088/2057-1976/2/2/025007>
- Azorin JFP, Saez J, Garcia LIR, Hernandez V. Investigation on the impact of the leaf trailing effect using the Halcyon integrated platform system. *Med Phys*. 2022;49:6161-6170. <https://doi.org/10.1002/mp.15833>

**How to cite this article:** Van Esch A, Kulmala A, Rochford R, Kauppinen J, Harju A. Testing of an enhanced leaf model for improved dose calculation in a commercial treatment planning system. *Med Phys*. 2022;49:7754–7765. <https://doi.org/10.1002/mp.16019>